Asociación Argentina
de Mecánica Computacional

Mecánica Computacional Vol XXXV, págs. 1231-1241 (artículo completo)
Martín I. Idiart, Ana E. Scarabino y Mario A. Storti (Eds.)
La Plata, 7-10 Noviembre 2017

RELIABILITY OF WOOD UTILITY POLES UNDER STOCHASTIC WIND LOAD AND MATERIAL CONSIDERING KNOTS

Laura V. González de Paz[a,b], **Diego A. García**[b,c] **and Marta B. Rosales**[a,b]

[a]*Department of Engineering, Universidad Nacional del Sur, Bahía Blanca, Argentina.*

[b]*CONICET, Argentina*

[c]*Department of Civil Engineering, Universidad Nacional de Misiones, Oberá, Argentina.*

Keywords: Wood poles, fragility curves, stochastic wind load, uncertain material properties, confidence bands.

Abstract. Wood utility poles are simple structures used in power networks and their failure may produce a significant impact on their reliability as well as economic consequences. Wind loads are one of the main causes of damage in wood utility poles. The present study addresses the dynamic behavior of Argentinean *Eucalyptus grandis* wood poles with uncertain material properties under stochastic wind load. Regarding the material, the lengthwise variability of the Modulus of Elasticity (MOE) and the second moment of area are simulated through the Weak Zone (WZ) model taking into account the knots presence. The stochastic wind velocity field is derived using the Spectral Representation Method (SRM) considering temporal and spatial correlation. Then, the wind load is obtained under the considerations of the Argentinean standard CIRSOC 102. The governing equations are discretized through the Finite Element Method (FEM). The stochastic analysis is performed by means of Monte Carlo Simulations (MCS). In this study, displacements are evaluated such that a percentage of damage is found for each wind velocity. Fragility curves are a useful means to evaluate the failure probability of the poles for a defined failure mode, under a given range of demand, here the wind load. The WZ model results are compared with other MOE models previously developed (as a random variable and as a random field through the Non Gaussian Karhunen-Loève Expansion). Also, confidence bands of the fragility curves are obtained for 95% of confidence.

1 INTRODUCTION

Wood utility poles are simple structures used in power networks and their failure can make a significant impact on the reliability as well as economic consequences, and the wind loads are one of the main loads that can cause damage. The probability of a structural failure is a function of both uncertainty in the capacity and uncertainty in the demand. The capacity of a structure to withstand a load is a function of its geometry and material properties. Although these quantities can be considered fixed, due to the natural origin of materials, uncertainties in material properties values are unavoidable. Among the existing tools, fragility curves can be useful to represent the probability of failure given a failure mode and a range of loads. In particular, it is a means to evaluate the behavior of structural systems. A study on the action of wind on industrial steel structures is reported in Palencia et al. (2008) which includes a wide inventory of usual typologies. Fragility curves of the complete structure as well as its components are obtained. *Eucalyptus grandis* is a wood extensively used in Argentina for structural purposes, in particular utility poles. Experimental studies are usually carried out to assess its properties and behavior (Piter et al., 2004) and more recently, computational approaches are reported (García et al., 2015). An experimental assessment of *Eucalyptus grandis* wood poles is contained in Torrán et al. (2009). A fragility study of wood poles including age deterioration is found in Shafieezadeh et al. (2014). To construct the dynamic wind load, the fluctuating wind component is obtained through the Spectral Representation Method (SRM) starting from a given Power Spectral Density Function (PSDF). The temporal and spatial correlations are taken into account by finding the cross-spectrum and introducing a coherence function (Shinozuka and Deodatis, 1991). The method yields a temporal record of the fluctuating wind velocity along the pole height. Combined with the standard recommendations, the fluctuating wind pressure is derived. This method was employed in the dynamic study of a guyed mast and tall buildings (Ballaben and Rosales, 2012; Castro et al., 2015).

The dynamic behavior of Argentinean *Eucalyptus grandis* wood poles with uncertain material properties under stochastic wind load is herein analyzed. The uncertain material properties are given by the variability of the Modulus of Elasticity (MOE) simulated by a stochastic process, through the Weak Zone model (WZ) taking into account the knots presence. To study the influence of the second area moment due to the presence of knots, this model is separated in two submodels: M1 or WZ_E-model with the MOE as a random field and M2 or WZ_{EI}-model with the MOE as a random field, now considering the influence of knots in the second area moment. A third model with the MOE value equal to deterministic mean value for whole length, is considered as a comparison model. The fragility curves are obtained from these material models for a given failure mode. Then, they are compared among them and with other MOE models previously developed in González de Paz et al. (2016) (as a random variable and as a random field through the Non Gaussian Karhunen-Loève Expansion). Results are numerically approximated by the Finite Element Method (FEM). Statistics of the response are obtained by means of Monte Carlo Simulations (MCS) with a previous convergence study carried out in order to determine the acceptable number of realizations. The model is discretized using the Finite Element Method (FEM). Also, confidence bands (CB) of the fragility curves are obtained for 95% of confidence. A confidence region is used in statistical analysis to represent the uncertainty in an estimate of a curve or function based on limited or noisy data. In Shinozuka et al. (2000), CB for fragility curves of damaged by earthquakes bridges are developed.

2 MODEL DESCRIPTION

2.1 Stochastic wind load

In order to calculate the dynamic stochastic wind load in the time domain, it is necessary to recreate a temporal record. This record is composed of two contributions: one is a fluctuating random variable with the position and time and other is a deterministic mean value with position variation.

The fluctuating wind velocity is obtained by the application of Spectral Representation Method (SRM) proposed by Shinozuka and Deodatis (1991). The method starts from a Power Spectral Density Function (PSDF) and a coherence function, to be chosen in accordance with the type of problem to be simulated. Then, the random signals are created as a superposition of harmonic functions with a random phase angle, weighed by coefficients that represent the importance of the value of frequency within the spectrum and the spatial correlation. Following the methodology developed in the reference work, a set of m gaussian stationary random processes $f_j^0(t), j = 1, 2, ...m$, with zero mean, $E[f_j^0(t)] = 0$, with a given cross spectral density matrix $S_0(\omega)$ where $S_{jk}^0(\omega) = F[R_{jk(\tau)^0}]$ are considered. $F[\,]$ represents the Fourier Transform operator and $R_{jk}^0(\tau)$ is the cross-correlation function $(j \neq k)$ or the autocorrelation function $(j = k)$. This matrix verifies $R_{jk}^0(\tau) = R_{jk}^0(-\tau)$ and then, $S^0(\omega)$ is a Hermitian and definite positive matrix. If the lower triangular matrix $H(\omega)$ is defined as a matrix whose Fourier transform exists, the relationship is

$$S^0(\omega) = H(\omega)\bar{H}^T(\omega) \tag{1}$$

where the bar stands for complex conjugate and the superscript T its transpose. The $F_j^0(t)$ process can be simulated by the following series:

$$f_j(t) = \sum_{k=1}^{3}\sum_{n=1}^{N}|H_{jk}(\omega_n)\mid \sqrt{2\Delta\omega}\cos[\hat{\omega}_n t + \theta_{kj}(\omega_n) + \Phi_{kn}] \tag{2}$$

where $\Delta\omega$ is the frequency interval with which the PSDF is discretized, $\omega_n = \Delta\omega(n-1)$, $\hat{\omega}_n = \omega_n + \psi_{kn}\Delta\omega$, ψ_{kn} is a random value uniformly distributed between 0 and 1, N is the amount of frequency ranges and, Φ_{kn} are the random independent phase angles uniformly distributed between 0 and 2π. If the values S_{jk} are all real, then the $\Theta_{jk}(\omega_n)$ are equal to zero. The decomposition represented by Eq.1 will be found by means of the *Cholesky Decomposition* of the spectral density matrix. The SRM requires of the implementation of different steps. The first one is the adoption of a Power Spectral Density Function (PSDF) and a coherence function. In this case, the PSDF suggested by Davenport is used (Dyrbye and Hansen (1996)):

$$R_N(z,\omega) = \frac{\omega S(z,\omega)}{\sigma^2(z)} = \frac{2}{3}\frac{f_L^2}{(1+f_L^2)^{4/3}} \tag{3}$$

where ω is the frequency in Hz, σ is the standard deviation and f_L is the non-dimensional frequency:

$$f_L = \omega\frac{L_u}{U(z)} \tag{4}$$

L_u is the length scale of turbulence (1200 m in Davenport's PSDF) and $U(z)$ is the wind mean velocity at height z. The expression for $U(z)$ correspond to the potential law adopted by the Argentinian stardard CIRSOC 102 (2005)

$$U(z) = 2.01V(z/z_g)^{2/\alpha} \tag{5}$$

where V is the nominal wind velocity which, together with z_g and α, are values given by the standard code depending on the characteristics of the structure location.

Then, the assumed coherence function is

$$Coh(z_i, z_j, \omega) = \exp\left\{-2\omega \frac{C_z \mid z_i - z_j \mid}{U(z_i) + U(z_j)}\right\} \tag{6}$$

where z_i and z_j are the heights of two given points of the pole. Then, each S_{ij} of the $S(\omega)$ matrix, for a given value of frequency can be calculated as

$$S_{ij}(z_i, z_j, \omega) = \sqrt{S(z_i, \omega) S(z_j, \omega)}\; Coh(z_i, z_j, \omega) \tag{7}$$

Following this procedure, each value $S_{ij}(z_i, z_j, \omega)$ will be calculated, and then, for each frequency ω, $H(\omega)$ matrices will be found. Finally, it is possible to construct the temporal series given by

$$u(z_j, t) = \sum_{k=1}^{m} \sum_{n=1}^{N} H_{jk}(\omega_n) \sqrt{2\Delta\omega}\, \cos[2\pi \hat{\omega}_n t + \Phi_{kn}]. \tag{8}$$

Table 1: Adopted values employed in the calculation of the time dependent velocity field.

Coefficients	σ^2	L_u	C_z	ω_c	$\Delta\omega$	t	Δt	N	m
Value	38.77	1200 m	11.5	2.5Hz	0.004 Hz	300 s	0.3 s	625	10

Once the fluctuating component of the wind speed has been determined, the Argentinean Standard CIRSOC 102 (2005), with some modifications carried out in order to take into account the dynamics of the wind, is employed in the calculation of the wind load. This standard defines the transversal wind force F as:

$$F = q_z\, G C_f A_f \tag{9}$$

where G is the gust-effect factor, C_f is the force coefficient which includes the effect of the shape of the structure, Af is the projected area normal to the wind. q_z is the dynamic velocity pressure evaluated at height z of the structure:

$$q_z = 0.613\, k_z\, k_{zt}\, k_d\, V^2 I \tag{10}$$

where k_z is the dynamic pressure exposure coefficient, k_{zt} is the topographic factor, k_d is the wind directionality factor, V is the basic wind speed and I is the importance factor. k_z is a function of the elevation z and the exposure category that described the ground surface roughness using information about the natural topography, vegetation and constructed facilities in the vicinity of the structure of interest.

For the determination of the fluctuating component of the wind velocity, the expression $k_z V = U(z)$ was used. Then, Eq. 10 becomes

$$\bar{q}_z = 0.613\, k_{zt}\, k_d (U(z) + u(z)) V\, I \tag{11}$$

and Eq. 9 results:

$$F = \bar{q}_z\, G C_f A_f \tag{12}$$

Table 2 shows the adopted values for the mentioned coefficients.

Table 2: Coefficients employed in the determination of the wind load according to CIRSOC 102 (2005).

Coefficients	G	C_f	I	k_d	k_{zt}	α	z_g
Value	0.85	2.0	1	0.85	1	9.5	274 m

2.2 Structural model

The structure under study is a *Eucalyptus grandis* pole which is modeled as a vertical column which diameter varies linearly, and embedded in the soil (Figure 1). The ground line distance from the base is equal to 1.8 m. The structural model is a beam clamped at the ground line subjected to wind load. The wind action is found using the method explained before, and the wood properties parameters and the geometric quantities (height and base and top diameters) were obtained from Torrán et al. (2009). The geometric quantities are depicted in Table 3.

Table 3: Geometric Data Torrán et al. (2009)

Height	GL-T distance	ground line diameter	top diameter
11.975 m	10.175 m	0.262 m	0.191 m

Damping in timber material is considered random with a uniform distribution, assuming values between 1% to 3% of the critical damping c_c. The mass is considered as a deterministic value equal to 707 kg/m^3, corresponding to the mean value reported by Torrán et al. (2009) for a mean moisture content of 45%.

The lengthwise variability of both the MOE and the second area moment of the pole cross section are simulated as stochastic processes, through the WZ model taking into account the knots presence. Then, this model results are compared with other MOE models previously developed in González de Paz et al. (2016).

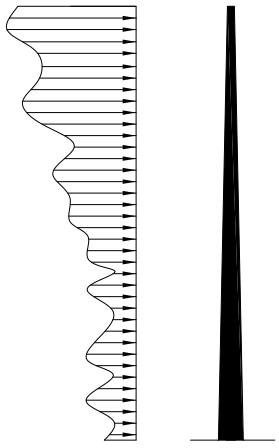

Figure 1: Structural scheme of pole and wind load.

2.2.1 Weak-zone model

In the weak-zone model, the structural timber component is modeled as a composite of short weak-zones connected by longer sections of clear wood. The length of the weak-zones are

proportional to five times the knot dimension. This feature was observed in the visual survey of the timber knots and the surrounding fibers. The MOE in each of these zones is constant and randomly assigned.

Reference values concerning the knots size in $Eucalyptus\ grandis$ poles are presented in Torrán et al. (2009). From this work, the mean value of this random variable and their interval are known. The application of the PME under the mentioned constrains leads to the truncated exponential PDF.

According to Torrán et al. (2009), the knots dimension in the lower segment of the pole has the following values: minimum 13 mm, mean 40 mm and maximum 100 mm. In the upper segment of the pole, the knots dimension has the following values: minimum 13 mm, mean 58 mm and maximum 100 mm. For the separation between knots, the PMF presented in García et al. (2016) is employed. This random variable has a mean value μ = 288.62 mm and standard deviation σ= 175.52 mm. The sample space ranges from 15 mm to 1040 mm.

The MOE values in this model are assigned randomly through their marginal PDF in function of the knot ratio (K) of each pole section, Table 4. The details may be found in García et al. (2016).

Table 4: Parameters of the gamma marginal PDF of the MOE for each value of K.

Parameters	K = 0	$0 <$ K$\leq 1/3$	$1/3 <$ K$\leq 2/3$	$2/3 <$ K
μ (GPa)	13.744	11.667	11.130	10.060
σ (GPa)	1.922	1.344	1.395	1.264

2.3 Confidence Bands

A Confidence Band (CB) is used in statistical analysis to represent the uncertainty in an estimate of a curve or function based on limited or noisy data. Confidence regions are closely related to Confidence Intervals (CI), which represent the uncertainly in an estimate of a single numerical value. While a CI only refers to a single point, a CB refers simultaneously to many points. The confidence level might be interpreted as the probability to find a CI that contain the real value of corresponding parameter (Neyman, 1937). The CB with 95% of confidence level is developed for each FC. The fragility curve line represents average value between the times the structure fails and total number of simulations for each value of wind velocity. The space between the upper and lower curves around the FC represents the CB, and the real FC would be there with a 95% of confidence level.

For the construction of CB, a CI for each point of wind velocity is found. A CI with a confidence level C is calculated as follow: The first step is to identify the mean value. Since the standard deviation is unknown, then the Student's t distribution is used as the critical value. The degree of freedom is found by subtracting one from the number of observations, $N - 1$. The critical value is found from the t-distribution table. In this table, the critical value is written as $t_\alpha(r)$, where r is the degree of freedom and $\alpha = (1 - C)/2$. Finally, the found values are:

$$CI = \left(\bar{x} - t_\alpha * \frac{s}{\sqrt{n}}, \bar{x} + t_\alpha * \frac{s}{\sqrt{n}} \right) \tag{13}$$

3 STUDY CASES

In order to perform the uncertainty quantification due to the stochastic modeling of the wind load and the MOE, the MOE lengthwise variability and of the second moment of the pole cross

section are simulated as stochastic processes, through the weak zone model taking into account the knots presence. To study the influence of the second area moment variation due to the presence of knots, this model is separated in two sub-models:

- M1 or WZ_E-model: the MOE lengthwise variability is simulated through the weak zone model taking into account the knots presence, but without considered their influence in the second area moment of the pole cross section.
- M2 or WZ_{EI}-model: the MOE lengthwise variability and of the second area moment, again as a stochastic process, through the weak zone model taking into account the knots presence, considering their influence in the second area moment of the pole cross section.

Results are compared with previous models (González de Paz et al., 2016):

- M3 or Det-model: the value of the MOE for the whole pole is considered deterministic and equal to the mean value presented in Torrán et al. (2009).
- M4 or Unif-model: the value of the MOE for the whole pole is simulated as a random variable through a gamma PDF, i.e. a uniform stochastic value.
- M5 or KL-model: the lengthwise variability of the MOE is represented with a random field through a Non Gaussian Karhunen-Loève Expansion with an exponential correlation function and a gamma marginal PDF.

A Monte Carlo method is used to perform the realizations within the Matlab environment with a number of realizations N= 1000 for each case. In all cases, the failure of the pole is assumed when the demand (displacement at the pole top) S is larger or equal to a given limit (maximum displacement allowed for this structural type) R, *i.e.* the probability of failure is written as

$$p_f = P[G(R, S) \leq 0] \tag{14}$$

where $G(\cdot)$ is known as the 'limit state function' and the probability of failure is identical with the limit state violation. In the this study, the limit is set when the displacement at the top of the pole (demand S) is equal or larger to a maximum displacement allowed for this structural type of $R = H/100$ (CIRSOC 601, 2011).

4 RESULTS

The structural deterministic problem governed by the Bernoulli-Euler beam equation is solved with a finite element discretization through FlexPDE, PDE (2017) software. A Monte Carlo method is used to perform the realizations within the Matlab environment with a number of 1000 simulations for each case.

Figure 2 shows the results of the analysis made for each study case. In Figure 2(a), the fragility curves (FCs) obtained for each case are presented. All FCs show their failure velocity range around a mean value where the curves intersected. The FCs derived for M1 and M2 models are equally widespread, but more widespread than M3 or deterministic model. M3 model curve is between M1 and M2 models. The M2 curve is on the left of M3 model. Its range of failure begins at a lower velocity than the other. This might be due to the fact that, the influence of the knots in the second moment of area is accounted for, and consequently these sections have the lowest stiffness in the pole.

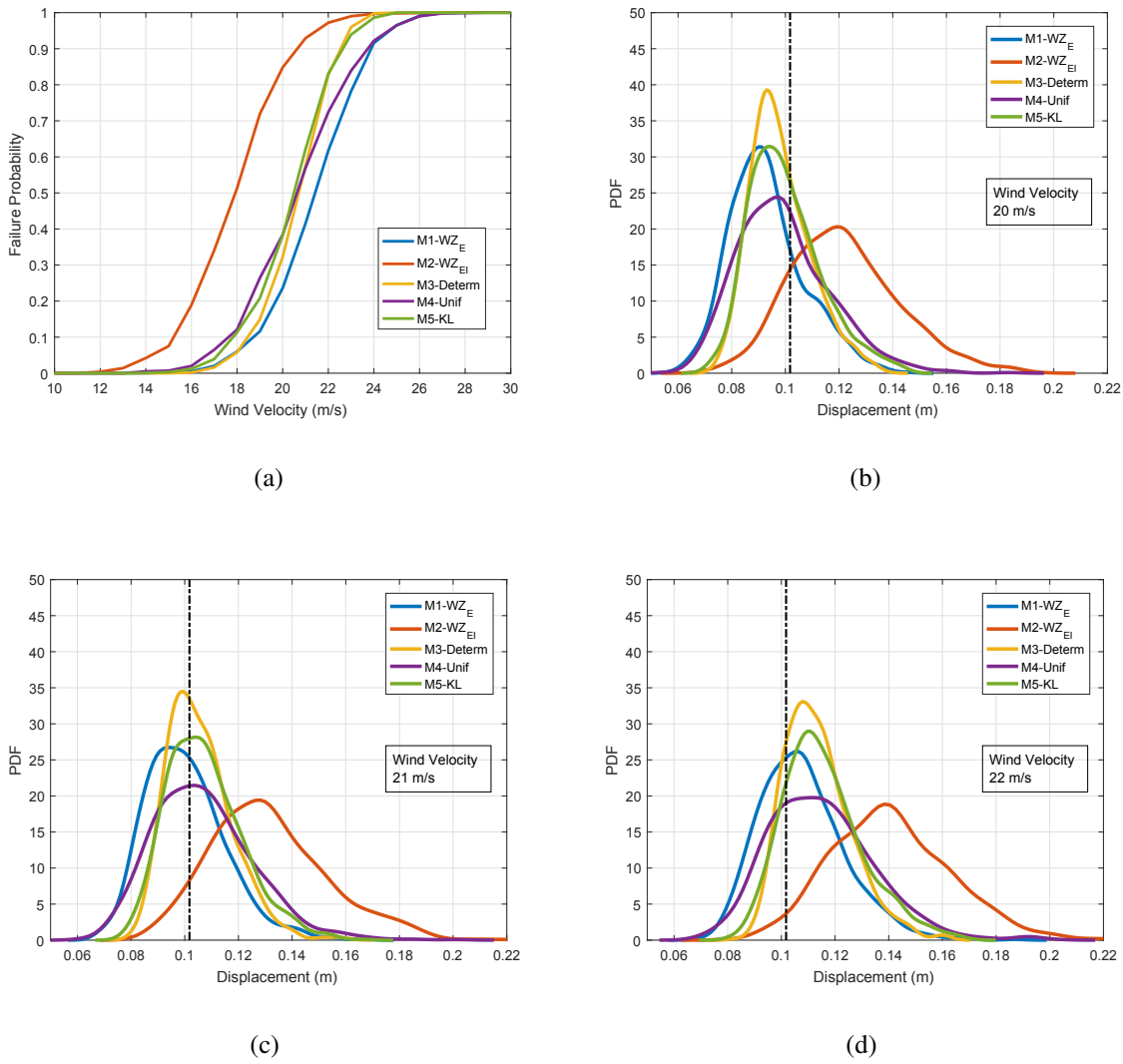

Figure 2: Top displacement of the pole. Three study cases. a) Fragility Curves; b) PDF for a wind velocity V = 20 m/s; c) PDF for a wind velocity V = 21 m/s; d) PDF for a wind velocity V = 22 m/s.

Figures 2(b-d) depict the PDF of the displacements at the pole top for the following wind velocities: 20 m/s (at the left of the intersection zone of Figure 2(a)), 21 m/s (within the intersection zone) and 22 m/s (at the right of the intersection zone). The displacement value adopted as "limit state" is indicated with a dashed line. The mode for almost all models is around the same value, but for M2 model, the mode is larger, showing that the M2 model is weakest model. Figures 3 (a) and (b) depict the mean values and Standard Deviations (SD) of the top displacements as functions of the wind velocity. Again, for M2 model, the mean values and the SD of displacements are larger than the other models. The first plot shows that M2 is weaker and the second plot shows that this model presents greater uncertainty.

Figure 4 shows the Confidence Bands (CB) of fragility curves obtained from the WZ models (M1 and M2) and the deterministic model (M3), with 95% of confidence level and the difference between the main curve and the upper and lower limit curves for each case. The maximum value of the difference is in each case at the inflection zone and has almost the same value between one case and another. Likewise, when analyzing the normal standard deviation for the inflection

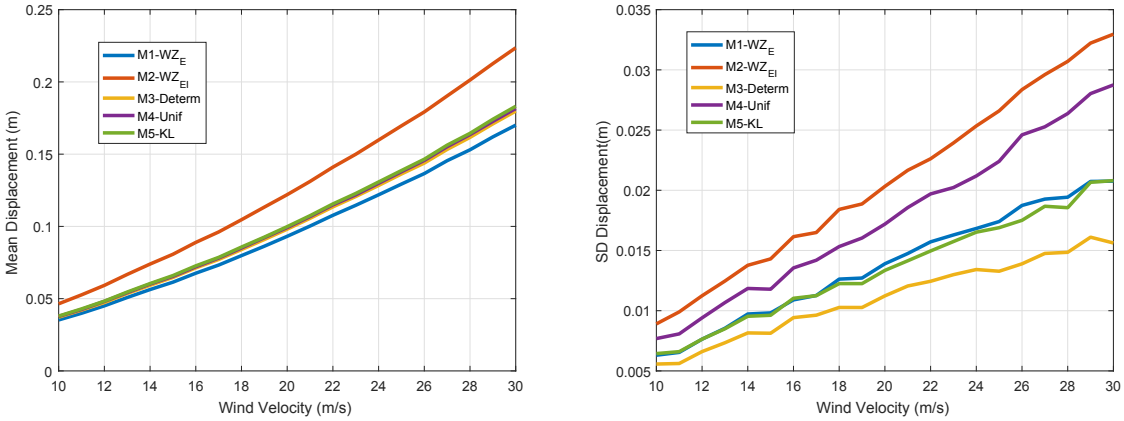

(a) (b)

Figure 3: Top displacement of the pole.a) Mean displacements; b) SD displacements.

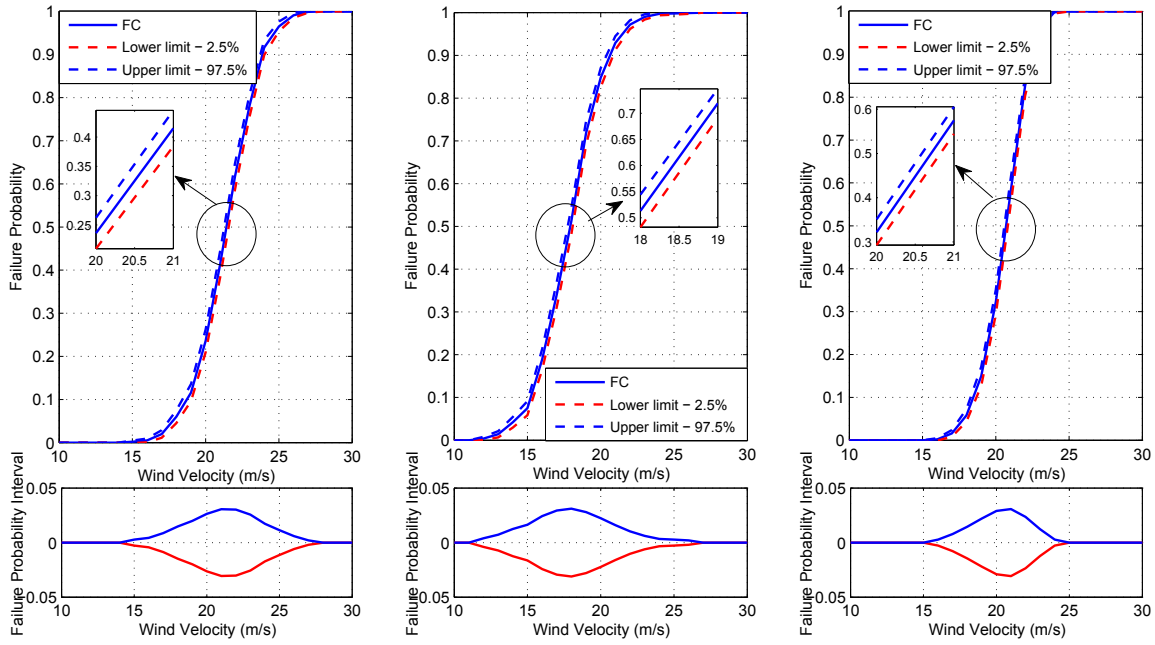

(a) (b) (c)

Figure 4: Confidence bands of fragility curves for 95% of confidence level. a) WZ model taking account only MOE variation (M1); b) WZ model taking account MOE and second moment area variation (M2); c) Deterministic model (M3).

point of each curve, a similar value is obtained. This maximum value that denotes the width of the CB depends on the size of the sample, being greater if the sample size is lower.

5 CONCLUSIONS

The structural behavior of wood utility poles under stochastic wind load and uncertain material properties was studied. The material uncertainty is represented with the Weak Zone model, a stochastic field simulation which takes into account the knots presence, in two variants: WZ_E-model without regard to the influence of knots in the second moment of area, but considering the MOE lengthwise variability (M1); WZ_{EI}-model in which the influence of knots is accounted for in the second area moment as well as in the MOE lengthwise variability (M2). Results of these models are compared with outcomes of previously developed material models: MOE as a deterministic mean value (M3), MOE as a random variable through a gamma PDF (M4) and MOE as a random field represented by a Non Gaussian Karhunen-Loève Expansion (M5).

All FCs show the failure wind velocity range around a mean value between M1-model and M2-model curves.

The range of failure of M2 curve begins at a lower wind velocity than in the rest of the models. The influence of knots in the MOE variability and in the second area moment are accounted for, and consequently, its global strength is lower. Also, the M2 model displacements results at the top show more dispersion than the other models. The results from the M2-model are rather different from the rest of the models, as was shown in the FCs, and in the analysis of displacements (mean value and standard deviation).

The maximum value in the confidence bands for all models is similar and is located at the inflection point in each FC. For the FCs, each iteration results in "fail" or "no fail", leading to a Bernoulli distribution. In this probability distribution, the SD is greater if the mean value is closer to 0.5. The inflection points in the FCs are around this value, then the SD and the CI will be greater. The width of the confidence bands depend on the size of the samples.

It would be necessary further analysis considering the influence of the random field of the second moment of area, leaving fixed the rest of the parameters in order to understand the results found with the stochastic material model M2.

REFERENCES

Ballaben J.S. and Rosales M.B. Parametric study of the dynamic along-wind response of a guyed tower. In *Proceedings of Segundo Congreso Latinoamericano de Ingeniería del Viento (CLIV2), La Plata, Argentina*. 2012.

Castro H., De Bortoli M., Paz R., and Marighetti J. Una metodología de cálculo para la determinación de la respuesta dinámica longitudinal de estructuras altas bajo la acción del viento. *Revista Internacional de Métodos Numéricos para Cálculo y Diseño en Ingeniería*, 31(4):235–245, 2015.

CIRSOC 102. *Reglamento Argentino de Acción del Viento sobre las Construcciones*. CIRSOC, 2005.

CIRSOC 601. *Proyecto de Reglamento Argentino de Estructuras de Madera CIRSOC 601*. INTI-CIRSOC, 2011.

Dyrbye C. and Hansen S.O. *Wind loads on structures*. John Wiley & Sons, 1996.

FlexPDE, PDE. Solutions inc. http://www. pdesolutions. com, 2017.

García D.A., Sampaio R., and Rosales M.B. Vibrational problems of timber beams with knots considering uncertainties. *Journal of the Brazilian Society of Mechanical Sciences and Engineering*, pages 1–13, 2015.

García D.A., Sampaio R., and Rosales M.B. Vibrational problems of timber beams with knots considering uncertainties. *Journal of the Brazilian Society of Mechanical Sciences and En-*

gineering, 38(8):2661–2673, 2016.

González de Paz L.V., A G.D., and Rosales M.B. Fragility curves of wood utility poles under stochastic wind load with material uncertain properties. In *Mecánica Computacional Vol XXXIV, Cordoba, Argentina*, pages 151–161. 2016.

Neyman J. Outline of a theory of statistical estimation based on the classical theory of probability. *Philosophical Transactions of the Royal Society of London. Series A, Mathematical and Physical Sciences*, 236(767):333–380, 1937.

Palencia A.J.G., Saffar A., and Godoy L.A. Curvas de fragilidad debidas a viento para edificaciones industriales metalicas. *Revista Internacional de Desastres Naturales, Accidentes e Infraestructura Civil*, 8(2), 2008.

Piter J., Zerbino R., and Blaß H. Visual strength grading of argentinean eucalyptus grandis. *Holz als Roh-und Werkstoff*, 62(1):1–8, 2004.

Shafieezadeh A., Onyewuchi U.P., Begovic M.M., and DesRoches R. Age-dependent fragility models of utility wood poles in power distribution networks against extreme wind hazards. *IEEE Transactions on Power Delivery*, 29(1):131–139, 2014.

Shinozuka M. and Deodatis G. Simulation of stochastic processes by spectral representation. *Applied Mechanics Reviews*, 44(4):191–204, 1991.

Shinozuka M., Feng M.Q., Lee J., and Naganuma T. Statistical analysis of fragility curves. *Journal of engineering mechanics*, 126(12):1224–1231, 2000.

Torrán E., Zitto S., Cotrina A., and Piter J.C. Bending strength and stiffness of poles of argentinean eucalyptus grandis. *Maderas. Ciencia y tecnología*, 11(1):71–84, 2009.